

Published in final edited form as:

Neurochem Int. 2007 May ; 50(6): 834–847.

Microarray Analysis of Oxidative Stress Regulated Genes in Mesencephalic Dopaminergic Neuronal Cells: Relevance to Oxidative Damage in Parkinson's Disease

Vellareddy Anantharam¹, Elin Lehrmann², Arthi Kanthasamy¹, Yongjie Yang¹, Probal Banerjee³, Kevin G. Becker⁴, William J. Freed², and Anumantha G. Kanthasamy¹

1 Parkinson Disorders Research Laboratory, Iowa Center for Advanced Neurotoxicology, Department of Biomedical Sciences, Iowa State University, Ames, IA, USA

2 Cellular Neurobiology Research Branch, National Institute on Drug Abuse, Intramural Research Program, National Institutes of Health, Department of Health and Human Services, Baltimore, MD, USA

3 City University of New York Staten Island, Department of Chemistry and Neuroscience Program, Staten Island, NY, USA

4 Gene Expression and Genomics Unit, Research Resources Branch, Intramural Research Program, National Institute on Aging, National Institutes of Health, Department of Health and Human Services, Baltimore, MD, USA

Abstract

Oxidative stress and apoptotic cell death have been implicated in the dopaminergic cell loss that characterizes Parkinson's disease. While factors contributing to apoptotic cell death are not well characterized, oxidative stress is known to activate an array of cell signaling molecules that participate in apoptotic cell death mechanisms. We investigated oxidative stress-induced cytotoxicity of hydrogen peroxide (H₂O₂) in three cell lines, the dopaminergic mesencephalon-derived N27 cell line, the GABAergic striatum-derived M213-20 cell line, and the hippocampal HN2-5 cell line. N27 cells were more sensitive to H₂O₂-induced cell death than M213-20 and HN2-5 cells. H₂O₂ induced significantly greater increases in caspase-3 activity in N27 cells than in M213-20 cells. H₂O₂-induced apoptotic cell death in N27 cells was mediated by caspase-3-dependent proteolytic activation of PKC δ . Gene expression microarrays were employed to examine the specific transcriptional changes in N27 cells exposed to 100 μ M H₂O₂ for 4 hrs. Changes in genes encoding pro- or anti-apoptotic proteins included up-regulation of BIK, PAWR, STAT5B, NPAS2, Jun B, MEK4, CCT7, PPP3CC and PSDM3, while key down-regulated genes included BNIP3, NPTXR, RAGA, STK6, YWHAH, and MAP2K1. Overall, the changes indicate a modulation of transcriptional activity, chaperone activity, kinase activity, and apoptotic activity that appears highly specific, coordinated and relevant to cell survival. Utilizing this *in vitro* model to identify novel oxidative stress-regulated genes may be useful in unraveling the molecular mechanisms underlying dopaminergic degeneration in Parkinson's disease.

Corresponding Author: Anumantha G. Kanthasamy, Ph.D, Eugene and Linda Lloyd Professor, Parkinson's Disorder Research Laboratory, Department of Biomedical Sciences, Iowa State University, 2062 Veterinary Medicine Building, Ames, IA 50011-1250, USA, Phone: (515) 294-2516, Fax: (515) 294-2315, E-mail: akanthas@iastate.edu

Publisher's Disclaimer: This is a PDF file of an unedited manuscript that has been accepted for publication. As a service to our customers we are providing this early version of the manuscript. The manuscript will undergo copyediting, typesetting, and review of the resulting proof before it is published in its final citable form. Please note that during the production process errors may be discovered which could affect the content, and all legal disclaimers that apply to the journal pertain.

Keywords

mitochondria; oxidative stress; gene expression; caspases; PKCdelta; Parkinson's disease

1. INTRODUCTION

The cellular mechanisms underlying selective loss of dopaminergic neurons in the substantia nigra associated with Parkinson's disease (PD) remain elusive (Dawson and Dawson 2003;Forman et al. 2004;Greenamyre and Hastings 2004;Jenner 2003;Moore et al. 2005;Tatton et al. 2003). Although apoptosis is considered to be an important mode of neuronal cell death in PD, cell signaling events leading to apoptotic cell death of nigral dopaminergic neurons are not fully understood. Recent studies indicate oxidative stress is a major initiator of cell death in PD (Dawson and Dawson 2003;Forman et al. 2004;Greenamyre and Hastings 2004;Jenner 2003;Moore et al. 2005;Tatton et al. 2003). Oxidative stress results from the generation of reactive oxygen species (ROS) or impairment of the cellular antioxidant system, which triggers a cascade of events leading to apoptosis, including mitochondrial dysfunction, cytochrome C release, impairment of the ubiquitin-proteasomal degradation system and iron metabolism, excitotoxicity and activation of multiple caspases and transcriptional factors (Abou-Sleiman et al. 2006;Beal 2005;Dawson and Dawson 2003;Forman et al. 2004;Greenamyre and Hastings 2004;Jenner 2003;Moore et al. 2005;Tan and Dawson 2006;Tatton et al. 2003).

Microarray-based gene expression analysis provides a powerful approach to unravel molecular mechanisms in neurodegenerative disease by identifying the simultaneous transcriptional regulation of thousands of genes (Bassilana et al. 2005;Dangond et al. 2004;Duke et al. 2006;Grunblatt et al. 2004;Mandel et al. 2003c;Miller and Federoff 2006;Nesic et al. 2002;Ricciarelli et al. 2004;Youdim 2003). Microarray-based gene expression profiling has been used by several labs to determine the effects induced by dopaminergic toxins MPTP and rotenone on spatial and temporal gene expression in animal and cell culture models of neurodegenerative disorders (Bassilana et al. 2005;Bonin et al. 2004;Chun et al. 2001;Duke et al. 2006;Graham et al. 2004;Grunblatt et al. 2004;Grunblatt et al. 2001;Mandel et al. 2003a;Mandel et al. 2003c;Miller et al. 2004;Miller and Federoff 2006;Napolitano et al. 2002;Youdim 2003). These and related gene expression studies suggest that alterations of several genes associated with the cell cycle and apoptosis are associated with dopaminergic neuronal degeneration. In this study, we used H₂O₂ as a direct inducer of oxidative insult and examined early changes in gene expression.

The mesencephalon is directly affected in Parkinson's disease. We therefore used the rat mesencephalon-derived N27 cell line, which represents a homogenous population of tyrosine hydroxylase-positive cells with functional characteristics resembling dopaminergic neurons (Prasad et al. 1998), as an *in vitro* model for studies of dopaminergic neurodegeneration (Anantharam et al. 2002;Kaul et al. 2003;Kitazawa et al. 2003;Yang et al. 2004). We have previously demonstrated that several dopaminergic toxins, including MMT, dieldrin, manganese and MPP⁺, all induce sequential proteolytic activation of caspase-3 and protein kinase C (PKC δ) followed by apoptotic cell death (Anantharam et al. 2002;Kaul et al. 2003;Kitazawa et al. 2003;Yang et al. 2004). We found that PKC δ is persistently activated as a result of the cleaved 41 kDa catalytic PKC δ fragment which subsequently promotes apoptotic cell death in N27 cells (Kanthasamy et al., 2003). In this study, we examined the H₂O₂-sensitivity of immortalized neuronal cell lines derived from different brain regions: a dopaminergic cell line (N27), a GABAergic cell line (M213-20), and a hippocampal cell line (HN2-5). These cell lines have been shown to retain a number of features that characterize the region and cell type from which they were derived (Anantharam et al. 2002;Giordano et al. 1993;Kaul et al. 2003;Kitazawa et al. 2003;Giordano et al. 1993;Prasad et al. 1998;Singh et

al. 1996). Therefore, the differential sensitivity of these individual cell lines to H₂O₂ may demonstrate truly different responses underlying the different mechanisms of susceptibility observed *in vivo*.

Presently we establish that, compared to the striatum-derived, GABAergic cell line M213-20 (Giordano et al. 1993), or the hippocampal cell line HN2-5, (Singh et al. 1996), the N27 cell line is highly sensitive to H₂O₂-induced oxidative stress and ensuing apoptotic cell death, and that activation of caspase-3 and PKC δ is involved in this process. Furthermore, we employed microarray gene expression profiling to examine the gene expression changes that accompany the apoptotic cascade using N27 cells exposed to a concentration of H₂O₂ known to cause oxidative stress and apoptotic cell death. Analysis of gene expression changes indicated that mitochondrial dysfunction, apoptosis, dopamine metabolism, transcriptional regulation and ubiquitin-proteasome degradation systems were strongly affected. The microarray data were validated for select genes and proteins using semi-quantitative PCR and Western blotting, respectively. Together with our previous findings, this presents a picture of mitochondrial dysfunction, with regulation of anti- and proapoptotic factors, and confirms that caspase-3-induced proteolytic activation of PKC δ is a key step in mediating apoptotic cell death in N27 cells.

2. METHODS

2.1. Cell culture

N27 cells were derived from rat mesencephalon and immortalized using a temperature-sensitive allele of the large simian virus 40 T antigen (Prasad et al. 1998), and then grown in RPMI medium supplemented with 10% fetal bovine serum, 1% L-glutamine, 100 U/ml penicillin and 100 U/ml streptomycin. HN2-5 cells were derived from mouse hippocampal neurons immortalized and cultured to about 70–80% confluence in DMEM containing 10% fetal bovine serum and penicillin-streptomycin (Singh et al. 1996). Both HN2-5 and N27 cells were maintained at 37°C in a humidified atmosphere of 5% CO₂. The GABAergic M213-20 cell line was derived from rat striatum and immortalized using a temperature-sensitive allele of the large simian virus 40 T antigen (Giordano et al. 1993), and grown in Dulbecco's modified Eagle's/F12 medium containing 10% fetal bovine serum, 2 mM L-glutamine, 50 u/ml penicillin, and 50 u/ml of streptomycin and incubated at 33°C in a humidified atmosphere containing 5% CO₂. Tissue culture media and supplements were purchased from InVitrogen, Carlsbad, CA.

2.2. Treatment paradigm

N27, HN2-5 and M213-20 cells were grown to 70–80% confluency and then exposed to 100–300 μ M H₂O₂ for 1–4 hrs. Cells were also pretreated with 50 μ M Z-DEVD-fmk or 2 μ M rottlerin prior to H₂O₂-treatment. Whenever possible, cells from the same treatment batch were simultaneously subjected to caspase-3 activity assay, western blot analysis, DNA fragmentation assay and total RNA extraction. All experiments were performed at least two times.

2.3. Cytotoxicity assays

Cytotoxicity assays were performed as described previously (Kaul et al., 2005). N27, M213-20 and HN2-5 cells were grown at similar cell densities in 24-well plates and simultaneously exposed to different concentrations of H₂O₂ (30–300 μ M) and 1 μ M of the cell-impermeable dye Sytox green® (Molecular Probes, Eugene, OR). Sytox green® enters dead cells and intercalates with DNA to produce a green fluorescent signal. The extent of cell death was quantified after 5 hrs, using the fluorescent reader with an excitation 485 nm and emission 538 nm.

2.4. Caspase-3 activity

Caspase-3 enzyme activity was determined as previously described (Kaul et al. 2003). Briefly, N27 and M213-20 cells were grown at similar cell densities in 24-well plates and were exposed to either 100 or 300 μ M H₂O₂. After a 3 hr exposure, cells were lysed and the resulting supernatants incubated with 50 μ M of the fluorescent caspase-3 substrate Ac-DEVD-AMC (MP Biomedicals, Irvine, CA) at 37°C for 1 hr. Caspase-3 activity was quantified using a fluorescence plate reader (excitation 380 nm, emission 460 nm; SpectraMax Gemini XS).

2.5. DNA fragmentation

DNA fragmentation was measured using a Cell Death Detection ELISA Plus Assay Kit (Roche Biochemicals, Indianapolis, IN) as described in our previous publications (Kaul et al. 2003). Briefly, N27 cells were grown at similar cell densities in 24-well plates and exposed to 100 μ M H₂O₂. The extent of DNA fragmentation was quantified in cell lysates after different exposure times in a Spectramax Microplate Reader (405 nm, blank reference 490 nm).

2.6. RNA extraction

Total RNA was extracted from N27 cells exposed to 100 μ M H₂O₂ for 4 hrs using TRIZOL[®] reagent (Invitrogen Ltd, Carlsbad, CA). A total of 2 \times 10⁶ cells were homogenized at 4°C in 0.5 ml TRIZOL[®] Reagent per the manufacturers' protocol. RNA pellets were gently air-dried, resuspended in RNase-free water and stored at -80°C. The quantity and quality of the RNA samples were examined spectrophotometrically and by formaldehyde agarose gel electrophoresis, demonstrating high-quality RNA with no evidence of smearing of ribosomal RNA or of high molecular weight bands indicative of DNA contamination.

2.7. Microarray experiments

In this study we employed the Human Focused Array, a membrane-based cDNA microarray containing 2700 different elements in duplicate, which can be accessed at <http://www.grc.nia.nih.gov/branches/rrb/dna/index/dnapubs.htm#2>. We used this human-focused cDNA array, as opposed to full chips, because the first generation, larger, commercially available "full" arrays were associated with significant hybridization problems. Furthermore, few, if any, well-characterized rat arrays were commercially available at the time. In contrast, we had extensive experience with the focused cDNA arrays for cross-species experiments, and we determined that the arrays were reliable for the study since the relatively long cDNAs used in these focused arrays allowed for good hybridization, even with occasional mismatches.

Radioactive labeling of RNA with ³³P-dCTP and hybridization assays were performed as described previously (Lehrmann et al. 2003). Briefly, 5 μ g total RNA was reverse transcribed in the presence of ³³P-labeled dCTP. The ³³P-labeled cDNA was purified through a spin column, denatured, and diluted in hybridization buffer and allowed to hybridize to the HFA for 16–18 h at 55°C with rotation. After hybridization, the arrays were rinsed once with 2XSSC buffer at room temperature, and twice at 60°C for 10 min with 2XSSC containing 0.1% SDS. The arrays were exposed to a low-energy phosphor screen (Molecular Dynamics) for 5 days and scanned in a Phosphoimager 860 (Molecular Dynamics) at 50 μ m resolution.

2.8. Z-scores and z-ratio

Raw hybridization intensity data were log-transformed and normalized to yield z-scores, which in turn were used to calculate a z-ratio value for each gene with respect to the H₂O₂-treated cells. The z-ratio was calculated as the difference between the observed gene z-scores for the experimental and the control comparisons, and dividing by the standard deviation associated with the distribution of these differences (Cheadle et al. 2003). Z-ratio values $\geq +2.0$ or ≤ -2.0 were chosen as cut-off values, defining increased and decreased expression, respectively.

2.9. Semi-Quantitative Polymerase Chain Reaction (QPCR)

Select changes in gene expression were examined by semi-QPCR. cDNA was prepared from the same RNA samples that were used for microarray analysis, and reverse transcription was performed using Superscript First-strand cDNA Synthesis System (Invitrogen, Carlsbad, CA). All procedures were carried out as per the manufacturer's protocol. Vector NTI software (version 1.2.6) was used to design oligonucleotide primers (Table 1), which were synthesized by Integrated DNA Technologies (Coralville, IA). Semi-QPCR was performed with first stand cDNA using Taq polymerase. Briefly, 1–2 μ g of total RNA was digested with DNase I at 65 $^{\circ}$ C for 15 min. The DNase I digest was then treated with dNTPs and oligo-dT for 5 min at 65 $^{\circ}$ C, and then incubated with the RT-enzyme (provided with the kit) for 1 hr at 42 $^{\circ}$ C and subsequently used in the PCR reaction. PCR was carried out in a 20 μ l reaction using appropriate primer sets with platinum Taq polymerase (Invitrogen, MD) as per manufacturer's instructions. The following PCR program was used: 95 $^{\circ}$ C 4 min, (95 $^{\circ}$ C 40s, 55 $^{\circ}$ C 30s and 70 $^{\circ}$ C, 45s)_n and 72 $^{\circ}$ C 5 min. The number of cycles (n) varied from 30–40. GAPDH and β -actin expression were used as internal controls. All PCR reactions were carried out in triplicate using a Thermo Hybaid PCR machine (Thermo Hybaid, Franklin, MA). PCR samples were then separated on 1% agarose gel. Images were captured with Kodak Image Station 2000MM (Kodak, Rochester, NY). The bands were quantified using the Kodak 1D (ver 3.6.2) software. Densitometric analysis of the bands obtained from untreated and H₂O₂-treated samples were normalized to respective GAPDH or β -actin message levels in the samples prior to comparison.

2.10. Western blotting

Changes in protein expression were also verified in Western blot experiments. Briefly, N27 cells in normal culture medium with serum were exposed to 100 μ M H₂O₂ as described in section 2.2. Cell extractions were performed as described previously (Kaul et al. 2003). Cell lysates containing equal amounts of protein were loaded in each lane and separated on a 10–12% SDS-PAGE gel (Kaul et al. 2003). Proteins were then transferred to a nitrocellulose membrane, and non-specific binding sites were blocked by treating with 5% non-fat dry milk powder for 2 hr. The membranes were then treated with primary antibodies (1: 1000 to 1:2000 dilution) directed against PKC δ , *PP2B*, NIP3, JunB, Stat5B and MEKK4 (Santa Cruz Biotechnology, Santa Cruz, CA) for 1 hr, followed by secondary HRP-conjugated anti-rabbit (1:2000) for 1 hr. Secondary antibody-bound proteins were detected using the ECL chemiluminescence kit (Amersham, Piscataway, NJ). To confirm equal protein loading, blots were reprobbed with a β -actin antibody (1:2000, Sigma-Aldrich, St. Louis, MO). Western blot images were captured with a Kodak 2000 MM imaging system (Kodak Inc., New Haven, CT). Western blot images are representative of data from at least 3 separate experiments.

3. RESULTS

3.1. H₂O₂-induced cytotoxicity in mesencephalic, striatal and hippocampal cell lines

The cytotoxicity of H₂O₂ on N27, M213-20 and HN2-5 cell lines was compared by exposing them to 30 μ M, 100 or 300 μ M H₂O₂ for 5 hr. As shown in Fig. 1, H₂O₂ treatment induced increases in cytotoxicity in N27 (317%, 373%, and 502%, respectively) and in M213-20 cells (131%, 179%, and 312%, respectively), whereas no or non-significant increases in cellular cytotoxicity was observed in HN2-5 cells (113%, 122%, and 136%, respectively). These results suggest that N27 cells were more sensitive to the oxidative insult by H₂O₂ than M213-20 or HN2-5 cells.

3.2. H₂O₂-induced increased caspase-3 activity in N27 and M213-20 cell lines

As oxidative stress initiates a caspase cascade that leads to apoptotic cell death, we examined whether H₂O₂ exposure would induce the activation of caspase-3 in N27 and M213-30 cells.

Caspase-3 activity was increased in both N27 and M213-20 cells after exposure to 100 or 300 μ M H₂O₂ for 3 hr (Fig. 2). Compared to untreated cells, N27 cells demonstrated increases in caspase-3 activity of 461% and 1071%, respectively, while the increases in M213-20 cells were only 106% and 147%, respectively. These results suggest that caspase-3 may be implicated in the H₂O₂-induced cytotoxicity in both N27 and M213-20 cells, and further demonstrate that N27 cells display a higher sensitivity to H₂O₂-induced increases in caspase-3 activity than is the case for M213-20 cells.

3.3. Caspase-3 mediates proteolytic activation of PKC δ in the N27 cell line

Recently, we showed that PKC δ , a member of the novel PKC isoform family, is a key substrate for caspase-3 and is proteolytically activated during apoptotic cell death induced by various dopaminergic toxins (Anantharam et al. 2002; Kanthasamy et al. 2003; Kaul et al. 2003; Kitazawa et al. 2003; Yang et al. 2004). Caspase-3-mediated proteolytic cleavage of native full-length PKC δ (74 kDa) results in the persistently activated catalytic fragment (41 kDa) and regulatory fragment (38 kDa), and the persistently activated cleaved catalytic PKC δ fragment promotes apoptotic cell death in dopaminergic clonal cells. As shown in Fig 3, treatment with 100 μ M and 300 μ M H₂O₂ for 4 hr induces proteolytic cleavage of PKC δ (72–74 kDa) into 38-kDa regulatory and 41-kDa catalytically active fragments in N27 dopaminergic neuronal cells. Pretreatment with the caspase-3-specific inhibitor Z-DEVD-FMK (50 μ M) significantly attenuated 100 μ M H₂O₂-induced proteolytic cleavage of PKC δ (Fig. 3), suggesting that caspase-3 cleaves PKC δ in dopaminergic N27 cells.

3.4. PKC δ mediates H₂O₂-induced apoptotic cell death in N27 cells

A quantitative DNA fragmentation assay was used to further confirm the results obtained by cytotoxicity assay. H₂O₂ treatment induced a time-dependent increase in DNA fragmentation in N27 cells (Fig. 4). Exposure to 100 μ M H₂O₂ for 1 hr, 3 hr and 4 hr resulted in 113%, 168% and 387% increases in DNA fragmentation compared to untreated N27 cells, respectively. We next examined the effect of the PKC δ -specific inhibitor rottlerin on DNA fragmentation during H₂O₂ treatment. As shown in Fig. 4, DNA fragmentation was significantly suppressed in N27 cells pretreated with 5 μ M rottlerin for 30 min prior to treatment with 100 μ M H₂O₂ for 4 hr compared to H₂O₂-treated cells. On the other hand rottlerin treatment alone did not significantly alter the basal DNA fragmentation level. These data suggest that oxidative stress-induced apoptotic cell death is in part mediated by proteolytically activated PKC δ .

3.5. Microarray analysis of gene expression in H₂O₂-treated N27 cells

As N27 cells were more sensitive to oxidative stress-induced apoptotic cell death than M213-20 cells, cDNA microarrays were employed to profile the gene expression changes in N27 cells exposed to 100 μ M H₂O₂ for 4 hrs. Gene expression was significantly altered by H₂O₂-treatment, with increases in sixty-five and decreases in forty-five candidate genes, respectively. We classified the candidate transcripts into groups associated with essential cellular functions, which demonstrated changes in genes encoding proteins associated with apoptosis, cell cycle and growth, chaperones, disease-related, mitochondria/redox, ubiquitin-proteasome system, nuclear/transcription, kinases, phosphatases, Ras/Rab related GTPases, and others (Table 2).

3.6. Semi-Quantitative PCR analysis of gene expression changes in H₂O₂-treated N27 cells

Select transcripts that were identified in the microarray analysis to be significantly changed following a 4 hr exposure to 100 μ M H₂O₂ were re-examined by semi-QPCR (Table 2). The human cDNA array provided results that could not be examined due to the limited availability of some corresponding rat sequences in GenBank. The semi-QPCR validated the gene expression changes for the six rat transcripts, Cyclin D1 (CCND1), signal transducer and activator of transcription 5b (STAT5b), Jun-B oncogene (JunB), PRKC, apoptosis, WT1,

regulator (PAWR), proteasome (prosome, macropain) 26S subunit, non-ATPase, 3 (PSMD3), and mitogen activated protein kinase kinase 1 (MAP2K1). An unchanged normalization transcript, glyceraldehyde-3-phosphate dehydrogenase (GAPDH) was also examined (Table 2). Semi-QPCR confirmed the increased gene expression for CCCND1, STAT5B, JunB, PAWR, and PSMD3 and decreased MAP2K1 gene expression in H₂O₂-treated cells.

3.7. Western blotting analysis of proteins whose gene expression was changed in H₂O₂-treated N27 cells

The lack of availability of specific antibodies detecting the rat proteins encoded by candidate genes limited our evaluation of all candidate genes. Five rat proteins, Jun-B, STAT5b, mitogen-activated protein kinase kinase 4 (MEKK4), protein phosphatase 3, catalytic subunit, beta isoform (PPP3C β), and the fBCL2/adenovirus E1B 19 kDa-interacting protein 3 (BNIP3), were examined (Table 3). Increases in JunB, STAT5b, MEKK4 and PPP3CC were observed at the protein level, as was the decrease in BNIP3 protein levels.

4. DISCUSSION

To better understand the selective degeneration of dopaminergic neurons in PD pathology, we studied the sensitivity of immortalized mammalian cell lines derived from the mesencephalon (N27, dopaminergic), striatum (M213-20, GABAergic) and hippocampus (HN2-5) to oxidative stress by exposing them directly to H₂O₂. H₂O₂ induced cytotoxic cell death in all three cell types; N27 cells were most sensitive and HN2-5 cells were least sensitive (N27>M213-20 and HN2-5). H₂O₂ treatment also induced increases in caspase-3 enzyme activity in N27 and M213-20 cells. GABAergic M213-20 cells were also less sensitive to H₂O₂-induced increases in caspase-3 enzymatic activity. Pretreatment with the caspase-3-specific inhibitor Z-DEVD-FMK significantly attenuated H₂O₂-induced proteolytic activation of PKC δ in N27 cells. Further, pretreatment with the PKC δ -specific inhibitor rottlerin significantly suppressed H₂O₂-induced DNA fragmentation in N27 cells. Taken together, our results suggest that mesencephalic dopaminergic N27 cells are more susceptible to H₂O₂-induced apoptotic cell death than striatal M213-20 and hippocampal HN2-5 cells. These results support the view that nigral dopaminergic neurons are highly vulnerable to oxidative damage.

To study the gene expression changes that accompany the oxidative stress-induced apoptotic cascade, microarray analysis was performed in N27 cells subjected to oxidative insult. The present study demonstrated that gene expression is significantly altered by H₂O₂ treatment, and we identified 65 primary candidate genes that were up-regulated and 45 candidate genes that were down-regulated. These genes were classified into groups associated with essential cellular functions including apoptotic cell death, mitochondrial dysfunction, transcriptional changes, second messenger systems, chaperone functions, ubiquitin-proteasome degradation, cell growth, and cytoskeletal architecture. The functional consequences of these select candidate genes are discussed below.

4.1. Proteasomal subunit 3 (PSMD3)

PSMD3 is a part of the 26S proteasome complex, which represents the most important site for protein degradation in eukaryotic cells, and consists of several components: the 20S multimeric complex containing the catalytic sites, an 11S proteasome activator, and the 19S regulatory particle (Ardley et al. 2004;Bossy-Wetzel et al. 2004). Recent evidence indicates that impairment of the ubiquitin-proteasome system, in addition to its established role in oxidative stress and mitochondrial dysfunction, may also contribute to the pathogenesis of PD (Dawson and Dawson 2003;Forman et al. 2004;Hattori and Mizuno 2004). Recently, gene defects in ubiquitin carboxyl-terminal esterase L1 (UCHL1), an enzyme linked to ubiquitination, and parkin have been noted. Microarray analysis revealed a 3-fold increase in Z-ratio of PSMD3

transcripts in H₂O₂-treated N27 cells (Table 2). These results were also confirmed by RT-PCR (Table 3). Therefore, oxidative stress-induced increases in PSDM3 levels may cause impairment of the ubiquitin-proteasome pathway during neuronal apoptosis.

4.2. Cyclin D1 (CCND1)

CCND1 is an important cell-cycle regulatory protein associated with cell proliferation and differentiation (Aguirre et al. 2004). CCND1 is thought to regulate the activities of Cdk4, Cdk6 and MEK-ERK, and its over-expression has been reported in several cancers and hematopoietic malignancies. Studies in experimental models suggest that Cdks and MAP-kinase may play roles in the pathogenesis of PD. Additionally, CCND1 has also been demonstrated to bind to several transcription factors and to modulate their transcriptional activity (Aguirre et al. 2004). In our study, microarray data revealed a 12-fold increase in the Z-ratio of CCND1 transcripts in H₂O₂ treated N27 cells (Table 2), which was supported by the 4.1-fold increase found by RT-PCR (Table 3), suggesting a role for CCND1 in oxidative stress-mediated dopaminergic cell death.

4.3. Bcl-2-interacting killer protein (BIK)

BIK is an apoptosis regulator belonging to the family of BH3-only proteins (Hur et al. 2004). The BH3-only members of the Bcl-2 protein family are essential for initiation of programmed cell death and stress-induced apoptosis. These proteins share the 9-amino acid BH3 region, which binds directly to the anti-apoptotic members of the Bcl-2 family and inhibits their apoptosis-suppressing function. Recently, BIK was demonstrated to play a role in stress-induced apoptosis, and suppression of BIK expression by siRNA protected cells from apoptotic cell death (Hur et al. 2004). Furthermore, BIK was strongly induced both at the mRNA and protein levels in estrogen starved cell models (Hur et al. 2004). We observed that H₂O₂ treatment induced a 4-fold increase in Z-ratio of BIK expression in microarray experiments (Table 2). Therefore, up-regulation of the BIK gene may render the dopaminergic cells vulnerable to oxidative stress, and suggests a pro-apoptotic role of BIK in oxidative stress-induced neuronal apoptosis.

4.4. Bcl-2/adenovirus E1B 19 kDa-interacting protein (BNIP3)

BNIP3 is an apoptosis regulator belonging to the Bcl-2 family of proteins (Crow 2002). Studies have shown BNIP3 plays a pivotal role in hypoxia- and ceramide-induced apoptotic cell death. BNIP3 expression is down-regulated in almost all pancreatic adenocarcinomas compared with normal pancreas (Crow 2002). Further, over-expression of the BNIP3 gene confers sensitivity of cells to apoptotic stimuli (Giatromanolaki et al. 2004). Our microarray analysis revealed that H₂O₂ treatment of N27 cells decreased the Z-ratio of BNIP3 by almost 3.8-fold (Table 2). These results were further validated by Western blot experiments demonstrating a 3-fold decrease in BNIP3 protein level (Table 4). Thus, the down-regulation of BNIP3 may suggest a pro-apoptotic role for BNIP3, and may represent a protective response of dopaminergic cells to overcome oxidative insult.

4.5. Mitogen-activated protein kinase kinase kinase 4 (MEKK4)

In mammalian cells, two families of stress-responsive MAPKs, JNK and p38, are activated by a variety of environmental stimuli including oxidative stress (Thomas and Haganir 2004). These MAPKs are activated by their cognate MAPK kinases (MAPKKs) and MAPKK kinases (MAPKKKs) through phosphorylation. MAP3K4 is one of the MAPKKKs that act upstream of JNK and p38. Recent studies have suggested a new mode of p38/JNK activation, which involves an interaction between GADD45 proteins and MAP3K4. MAP3K4 has also been shown to interact with 14-3-3 proteins (Thomas and Haganir 2004). Microarray analysis revealed an increase in Z-ratio by 3.8-fold in MEKK4 mRNA levels in H₂O₂-treated N27

cells (Table 2). These results were further confirmed by a 3.6-fold increase in protein expression as determined by Western blot experiments (Table 4). Overall, H₂O₂-induced increases in both mRNA and protein levels for MEKK4 suggest a key role for this kinase in oxidative stress-induced apoptotic cell death of neuronal cells.

4.6. PKC apoptosis WT1 regulator (PAWR)

PAWR is a Wilms tumor 1 (WT1)-interacting protein which suppresses WT1 transcription factor function via physical interaction, resulting in deregulated cell growth and tumorigenesis (Johnstone et al. 1998). PAWR has been demonstrated to induce apoptosis in different cell types and is up-regulated in rat prostate cells undergoing apoptosis, while over-expression of PAWR confers enhanced sensitivity to apoptotic stimuli. Recently, PAWR has also been shown to inhibit the activity of the atypical PKC isoforms by physically interacting with these proteins (Moscat and Diaz-Meco 2003). As shown in Table 4, exposure to H₂O₂ increased the Z-ratio of PAWR gene by almost 4-fold in microarray experiments (Table 2). These results were confirmed in RT-PCR experiments where we observed a 3-fold increase in PAWR mRNA levels (Table 3). Our results suggest that PAWR is a pro-apoptotic protein and renders the dopaminergic cells vulnerable to oxidative stress.

4.7. Signal transducer and activator of transcription 5b (STAT5B)

STAT5B activity is induced by a number of cytokines and growth factors, resulting in transcriptional activation of specific target genes (Baskiewicz-Masiuk and Machalinski 2004). STAT5B plays an important role in a variety of cellular processes, including proliferation, differentiation, and apoptosis (Baskiewicz-Masiuk and Machalinski 2004). Aberrant regulation of STAT5 has been observed in solid tumors as well as in patients with either chronic or acute myeloid leukemia (Merghoub et al. 2001). Dominant-negative STAT5B has recently been shown to inhibit tumor growth and induces apoptosis in T47D-derived tumors in nude mice. Therefore, STAT5B is considered to be a survival factor (Yamashita et al. 2004). STAT1 was recently shown to mediate etoposide-induced apoptosis in HeLa cells (Devries et al. 2004). In our microarray experiments with N27 cells treated with H₂O₂, we observed that STAT5B was up-regulated by a z-ratio of 4 (Table 2). A 3-fold increase in mRNA level (Table 3) and 2.5-fold increases in protein levels (Table 4) were obtained from semi-quantitative RT-PCR and Western blot experiments respectively confirming the microarray data. These data suggest that STAT5B may play an anti-apoptotic role in oxidative stress-induced apoptotic cell death.

4.8. JunB proto-oncogene (JunB)

JunB is a member of the activator protein-1 (AP-1) family of transcription factors and over-expression of JunB protects against axotomy-induced nigral cell death (Winter et al. 2002). JunB appears to function as a negative regulator of a number of cell systems, including proliferation, cell cycle progression and cell survival (Pietro and Zauli 2004). In M1 mouse myeloid leukemia cells, induction of differentiation with either chemicals or cytokines is associated with an increase in *junB* expression (Pietro and Zauli 2004). In this study, microarray analysis revealed an increase in JunB expression by a z-ratio of 4 after exposure to H₂O₂ (Table 2). Microarray results were confirmed with RT-PCR and Western blot analysis, which revealed a 2.8-fold increase in mRNA and a 3-fold increase in protein levels in H₂O₂-treated N27 cells (Tables 3 and 4). Our data therefore suggest that JunB may play an important role in oxidative damage in dopaminergic cells.

4.9. Protein phosphatase 2B (PP2B)

PP2B is a member of the protein phosphatase (PP) family of proteins involved in the dephosphorylation of serine and threonine residues. In general, the phosphatase holoenzyme

is a trimeric complex composed of a regulatory subunit, a variable subunit and a catalytic subunit. Four major families of protein phosphatase catalytic subunits have been identified, designated PP1, PP2A, PP2B (calcineurin) and PP2C (Strack et al. 2004). Calcineurin is a calcium-dependent serine/threonine protein phosphatase that is highly expressed in the CNS and has been implicated in neurodegenerative disorders including PD (Tatton et al. 2003; Wu et al. 2004). Recently, the PP2B gene was identified as a potential schizophrenia susceptibility gene, supported by the idea that alterations in PP2B signaling contribute to schizophrenia pathogenesis (Gerber et al. 2003). Recent studies have shown the decrease in DARPP-32 Thr34 phosphorylation was mediated through Ca²⁺-dependent activation of the Ca²⁺-calmodulin-dependent phosphatase, PP2B in the neostriatal neurons (Nishi et al. 2002). In contrast, the decrease in Thr75 phosphorylation was mediated through Ca²⁺-dependent activation of dephosphorylation by protein phosphatase-2A. The results provide support for a complex effect of glutamate on dopaminergic signaling through the regulation of dephosphorylation of different sites of DARPP-32 by different protein phosphatases. Analysis of microarray data revealed a 3.0-fold increase in the Z-ratio of PP2B expression after H₂O₂ treatment (Table 2). Western blot analysis revealed a 2.3-fold increase in protein levels in H₂O₂-treated N27 cells (Table 4). Our data therefore suggest that PP2B may play a critical role in oxidative stress-induced dopaminergic cell death.

4.10. Neuronal PAS domain protein 2 (NPAS2)

NPAS2 has been postulated to be a carbon dioxide and nitric oxide-responsive transcription factor implicated in circadian rhythm regulation (Gilles-Gonzalez and Gonzalez 2004). Nitric oxide knockout animals were resistant to Parkinsonian toxin MPTP-induced dopaminergic cell death and neuronal nitric oxide inhibitor protects against MPTP neurotoxicity (Grunewald and Beal 1999). In this study, we found a 5.3-fold increase in the Z-ratio of NPAS2 mRNA levels in response to H₂O₂ exposure (Table 2), suggesting this heme-binding NPAS2 transcription factor may play a role in H₂O₂-induced apoptotic cell death of dopaminergic cells.

4.11. Myeloid cell leukemia-1 (MCL-1)

MCL-1 is an anti-apoptotic Bcl-2 family protein which prevents apoptosis by maintaining the integrity of the mitochondrial membrane, thereby preventing the release of cytochrome C, activation of caspases and DNA fragmentation (Zhuang and Brady 2006). In this study, we observed that H₂O₂-treatment induced an increase by a z-ratio of 4 in the expression of the MCL-1 gene in microarray experiments (Table 2). Therefore, up-regulation of the MCL-1 gene may suggest an anti-apoptotic response of dopaminergic cells to oxidative insult and an anti-apoptotic role of MCL-1 in oxidative-stress-induced neuronal apoptosis.

4.12. Suppressor of Ty4 homolog 1 (Supt4H1)

Supt4H1 interacts with histones to assemble a repressive chromatin structure, important for the formation and/or maintenance of chromatin structure (Bolton and Boeke 2003). Therefore, the down-regulation of Supt4H1 mRNA by a z-ratio of -5.5 observed in this study could influence the loss of chromatin structure, which may have contributed to the chromatin condensation observed during H₂O₂-induced dopaminergic apoptosis (Table 2).

4.13. Synuclein beta (SNCB)

The synuclein family consists of three isoforms termed α , β and γ . α -Synuclein, but not β - or γ -synucleins, accumulate in various pathological lesions in neurodegenerative disorders, such as Parkinson's disease (PD), dementia with Lewy bodies (DLB) and multiple system atrophy, which are collectively termed alpha-synucleinopathies (Von Bohlen Und Halbach 2004). Previously, we showed that α -synuclein over-expression protects against MPP⁺ neurotoxicity (Kaul et al. 2005). Also, MPTP induced a down-regulation of α -synuclein, but did not affect

regulation of β -synuclein or parkin, in the murine substantia nigra (Xu et al. 2005). Additionally, α -synuclein-derived peptides that blocked α -synuclein aggregation were able to protect against oxidative stress in transgenic animal models of PD, suggesting that loss of the α -synuclein regulation may result in cell death. The observed down-regulation of β -synuclein (z-ratio = -3.8) may initiate α -synuclein aggregation and contribute to dopaminergic cell death (Table 2).

4.14. Chaperonin-containing TCP1 protein (CCT7)

CCT7 is a eukaryotic chaperonin, which is part of a hetero-oligomeric complex that facilitates the proper folding of tubulin, actin and contractin. Alterations in the gene expression of the structural proteins actin and tubulin have recently been reported in MPTP-induced dopaminergic degeneration (Cairns et al. 2004;Przedborski and Vila 2003). We observed an approximately 6-fold increase in the z-ratio of CCT7 by microarray analysis (Table 2), suggesting that the chaperone activity of CCT7 may be important for oxidative stress-induced neuronal apoptosis.

4.15. Tyrosine 3-monooxygenase/tryptophan 5-monooxygenase activation protein, eta polypeptide (YWHAH)

YWHAH, or 14-3-3 eta (14-3-3 η) is a member of the dimeric 14-3-3 family of signal transduction proteins that specifically binds to phosphorylated serine on a variety of signaling molecules (Berg et al. 2003;Ubl et al. 2002). The 14-3-3 proteins are most abundantly expressed in the brain, are important for cell survival and have an inhibitory effect on apoptosis. Most of the 14-3-3 isoform proteins act as chaperones, and control the subcellular localization of the binding partners. Upon binding, they target them to their protein partners, and stimulate protein-protein interactions with other signaling proteins. 14-3-3 proteins have been shown to play a role in various physiological cellular processes such as signaling, cell growth, division, adhesion, differentiation, apoptosis, cell survival and regulation of ion channels. More than 100 binding partners for 14-3-3 proteins have been discovered, including proteins that are associated with dopaminergic degeneration such as apoptotic cell signaling proteins, BAD, Bcl-2, Bax, protein kinases, TH and DAT (Ostrerova et al. 1999). In this study, we observed a down-regulation of YWHAH (z-ratio = -2.9) by microarray analysis (Table 2), indicating that loss of the chaperone activity of YWHAH may play a role in oxidative signaling underlying oxidative damage in dopaminergic neurons.

4.16. Functional significance of oxidative stress and gene expression profiles

In recent years, studies have reported gene expression profiles for MPTP- and oxidative stress-induced dopaminergic cell death in animal and cell culture models of Parkinson's disease; however, no consistent gene expression patterns have been identified by these studies (Bassilana et al. 2005;Bonin et al. 2004;Chun et al. 2001;Conn et al. 2002;Duke et al. 2006;Grunblatt et al. 2004;Grunblatt et al. 2001;Holtz and O'Malley 2003;Kuhn et al. 2003;Mandel et al. 2003b;Mandel et al. 2003c;Miller et al. 2004;Miller and Federoff 2006;Napolitano et al. 2002;Xu et al. 2005;Yoo et al. 2004;Youdim 2003;Youdim et al. 2002). The different results obtained from profiling gene expression in dopaminergic cells or regions could be attributed to differences in model systems, microarray templates, time, doses and dopaminergic toxins used. However, a pattern of affected genes with specific functions has emerged in several studies. In general, the affected genes participate in iron regulation, MAP kinases signaling, chaperone activity, mitochondrial dysfunction, nuclear proteins associated with chromatin structure, DNA-repair enzymes, impairment of the ubiquitination and proteasomal degradation system and DNA-repair enzymes. Our studies are in line with these findings, suggesting that the H₂O₂-induced alterations in the dopaminergic cell line studied resulted in altered expression of both pro- and anti-apoptotic proteins, mitochondrially-

related proteins, transcription factors including heme-binding transcription factors, proteins associated with proteasomal degradation, molecular chaperones, MAP kinases, (tyrosine kinases, phosphatases) and nuclear proteins associated with chromatin structure, and DNA-repair enzymes. The combined effect of changes in different gene cascades may set the stage for the development and progression of apoptosis in dopaminergic neurons during oxidative insult.

In conclusion, we demonstrate that dopaminergic mesencephalic cells (N27) are more sensitive to oxidative stress-induced apoptotic cell death as compared to GABAergic striatal cells or hippocampal cells. The observed differences in susceptibility of these three cell lines to H₂O₂ cannot be exclusively attributed to immortalization procedures or species differences, because previous studies have shown that oxidative stress-mediated cell death mechanisms are very similar in dopaminergic cell lines that have been derived from different species and immortalized by different procedures, i.e., the rat N27 cell line (Kaul et al. 2003), the mouse MN9D cell line (Choi et al. 1999; Nicotra and Parvez 2002), and human SH-SY5Y cells (Gomez et al. 2001). The neurochemical properties of these cells may account for the differential sensitivity to oxidative damage. In particular, dopamine-containing neuronal cells show enhanced susceptibility to oxidative damage (Kweon et al. 2004; Kitazawa et al. 2002). Together with our previous findings, we have shown that mitochondrial dysfunction, induction of anti- and pro-apoptotic factors, and in particular, caspase-3-induced proteolytic activation of PKC δ , all mediate H₂O₂-induced apoptotic cell death in N27 cells. Furthermore, these results occurred in the same population of cells that were used for microarray experiments. Thus, the gene expression changes measured in microarray are occurring simultaneously with the apoptotic cell death events. Future studies should compare differential gene expression in the M213-20 striatal cell line and the N27 mesencephalic cell line to elucidate the molecular mechanisms underlying cell type-specific oxidative damage.

By employing microarray, RT-PCR and Western blotting analysis, we have identified several oxidative stress-regulated genes associated with specific cellular functions in the dopaminergic N27 cell line. While the picture of gene regulation in PD is far from complete, further functional characterization of the affected genes and their protein products may provide insights into the molecular pathological mechanisms associated with oxidative stress-induced dopaminergic degeneration. Inclusion of comparative gene expression profiling analysis of *in vitro* and *in vivo* neurotoxic and transgenic PD models also greatly aid in identifying key pathways associated with the neurodegenerative process in PD. This information will ultimately lead to novel molecular drug targets for intervention in the oxidative stress-induced dopaminergic cell loss observed in Parkinson's disease as well as in other neurodegenerative disorders, including cerebral ischemia, amyotrophic lateral sclerosis and even certain types of drug abuse-related neurotoxic conditions, in which oxidative stress contributes significantly to the disease etiology, process and/or outcome (Cadet et al. 2003; Imam et al. 2002; Jayanthi et al. 2004).

Acknowledgements

This study was supported by NIH grants NS 45133, ES 10586, NS 386644 and the Intramural Research Programs of the NIDA and the NIA, NIH, DHHS. The authors also gratefully acknowledge Mr. William H. Wood, GEGU, NIA IRP, NIH, DHHS and Dr. Siddharth Kaul for their technical assistance.

References

- Abou-Sleiman PM, Muqit MM, Wood NW. Expanding insights of mitochondrial dysfunction in Parkinson's disease. *Nat Rev Neurosci* 2006;7(3):207–219. [PubMed: 16495942]
- Aguirre D, Boya P, Bellet D, Faivre S, Troalen F, Benard J, Saulnier P, Hopkins-Donaldson S, Zangemeister-Wittke U, Kroemer G, Raymond E. Bcl-2 and CCND1/CDK4 expression levels predict the cellular effects of mTOR inhibitors in human ovarian carcinoma. *Apoptosis* 2004;9(6):797–805. [PubMed: 15505422]

- Anantharam V, Kitazawa M, Wagner J, Kaul S, Kanthasamy AG. Caspase-3-dependent proteolytic cleavage of protein kinase Cdelta is essential for oxidative stress-mediated dopaminergic cell death after exposure to methylcyclopentadienyl manganese tricarbonyl. *J Neurosci* 2002;22(5):1738–1751. [PubMed: 11880503]
- Ardley HC, Scott GB, Rose SA, Tan NG, Robinson PA. UCH-L1 aggresome formation in response to proteasome impairment indicates a role in inclusion formation in Parkinson's disease. *J Neurochem* 2004;90(2):379–391. [PubMed: 15228595]
- Baskiewicz-Masiuk M, Machalinski B. The role of the STAT5 proteins in the proliferation and apoptosis of the CML and AML cells. *Eur J Haematol* 2004;72(6):420–429. [PubMed: 15128421]
- Bassilana F, Mace N, Li Q, Stutzmann JM, Gross CE, Pradier L, Benavides J, Menager J, Bezdard E. Unraveling substantia nigra sequential gene expression in a progressive MPTP-lesioned macaque model of Parkinson's disease. *Neurobiol Dis* 2005;20(1):93–103. [PubMed: 16137570]
- Beal MF. Mitochondria take center stage in aging and neurodegeneration. *Ann Neurol* 2005;58(4):495–505. [PubMed: 16178023]
- Berg D, Holzmann C, Riess O. 14-3-3 proteins in the nervous system. *Nat Rev Neurosci* 2003;4(9):752–762. [PubMed: 12951567]
- Bolton EC, Boeke JD. Transcriptional interactions between yeast tRNA genes, flanking genes and Ty elements: a genomic point of view. *Genome Res* 2003;13(2):254–263. [PubMed: 12566403]
- Bonin M, Poths S, Osaka H, Wang YL, Wada K, Riess O. Microarray expression analysis of gad mice implicates involvement of Parkinson's disease associated UCH-L1 in multiple metabolic pathways. *Brain Res Mol Brain Res* 2004;126(1):88–97. [PubMed: 15207921]
- Bossy-Wetzel E, Schwarzenbacher R, Lipton SA. Molecular pathways to neurodegeneration. *Nat Med* 2004;(10 Suppl):S2–9. [PubMed: 15272266]
- Cadet JL, Jayanthi S, Deng X. Speed kills: cellular and molecular bases of methamphetamine-induced nerve terminal degeneration and neuronal apoptosis. *Faseb J* 2003;17(13):1775–1788. [PubMed: 14519657]
- Cairns NJ, Lee VM, Trojanowski JQ. The cytoskeleton in neurodegenerative diseases. *J Pathol* 2004;204(4):438–449. [PubMed: 15495240]
- Cheadle C, Vawter MP, Freed WJ, Becker KG. Analysis of microarray data using Z score transformation. *J Mol Diagn* 2003;5(2):73–81. [PubMed: 12707371]
- Choi WS, Canzoniero LM, Sensi SL, O'Malley KL, Gwag BJ, Sohn S, Kim JE, Oh TH, Lee EB, Oh YJ. Characterization of MPP(+)-induced cell death in a dopaminergic neuronal cell line: role of macromolecule synthesis, cytosolic calcium, caspase, and Bcl-2-related proteins. *Exp Neurol* 1999;159(1):274–282. [PubMed: 10486196]
- Chun HS, Gibson GE, DeGiorgio LA, Zhang H, Kidd VJ, Son JH. Dopaminergic cell death induced by MPP(+), oxidant and specific neurotoxicants shares the common molecular mechanism. *J Neurochem* 2001;76(4):1010–1021. [PubMed: 11181820]
- Conn KJ, Gao WW, Ullman MD, McKeon-O'Malley C, Eisenhauer PB, Fine RE, Wells JM. Specific up-regulation of GADD153/CHOP in 1-methyl-4-phenyl-pyridinium-treated SH-SY5Y cells. *J Neurosci Res* 2002;68(6):755–760. [PubMed: 12111836]
- Crow MT. Hypoxia, BNip3 proteins, and the mitochondrial death pathway in cardiomyocytes. *Circ Res* 2002;91(3):183–185. [PubMed: 12169642]
- Dangond F, Hwang D, Camelo S, Pasinelli P, Frosch MP, Stephanopoulos G, Brown RH Jr, Gullans SR. Molecular signature of late-stage human ALS revealed by expression profiling of postmortem spinal cord gray matter. *Physiol Genomics* 2004;16(2):229–239. [PubMed: 14645737]
- Dawson TM, Dawson VL. Molecular pathways of neurodegeneration in Parkinson's disease. *Science* 2003;302(5646):819–822. [PubMed: 14593166]
- Devries TA, Kalkofen RL, Matassa AA, Reylund ME. Protein Kinase C{delta} Regulates Apoptosis via Activation of STAT1. *J Biol Chem* 2004;279(44):45603–45612. [PubMed: 15322115]
- Duke DC, Moran LB, Kalaitzakis ME, Deprez M, Dexter DT, Pearce RK, Graeber MB. Transcriptome analysis reveals link between proteasomal and mitochondrial pathways in Parkinson's disease. *Neurogenetics* 2006;7(3):139–148. [PubMed: 16699787]
- Forman MS, Trojanowski JQ, Lee VM. Neurodegenerative diseases: a decade of discoveries paves the way for therapeutic breakthroughs. *Nat Med* 2004;10(10):1055–1063. [PubMed: 15459709]

- Gerber DJ, Hall D, Miyakawa T, Demars S, Gogos JA, Karayiorgou M, Tonegawa S. Evidence for association of schizophrenia with genetic variation in the 8p21.3 gene, PPP3CC, encoding the calcineurin gamma subunit. *Proc Natl Acad Sci U S A* 2003;100(15):8993–8998. [PubMed: 12851458]
- Giatromanolaki A, Koukourakis MI, Sowter HM, Sivridis E, Gibson S, Gatter KC, Harris AL. BNIP3 expression is linked with hypoxia-regulated protein expression and with poor prognosis in non-small cell lung cancer. *Clin Cancer Res* 2004;10(16):5566–5571. [PubMed: 15328198]
- Gilles-Gonzalez MA, Gonzalez G. Signal transduction by heme-containing PAS-domain proteins. *J Appl Physiol* 2004;96(2):774–783. [PubMed: 14715687]
- Giordano M, Takashima H, Herranz A, Poltorak M, Geller HM, Marone M, Freed WJ. Immortalized GABAergic cell lines derived from rat striatum using a temperature-sensitive allele of the SV40 large T antigen. *Exp Neurol* 1993;124(2):395–400. [PubMed: 8287936]
- Gomez C, Reiriz J, Pique M, Gil J, Ferrer I, Ambrosio S. Low concentrations of 1-methyl-4-phenylpyridinium ion induce caspase-mediated apoptosis in human SH-SY5Y neuroblastoma cells. *J Neurosci Res* 2001;63(5):421–428. [PubMed: 11223917]
- Graham RM, Frazier DP, Thompson JW, Haliko S, Li H, Wasserlauf BJ, Spiga MG, Bishopric NH, Webster KA. A unique pathway of cardiac myocyte death caused by hypoxia-acidosis. *J Exp Biol* 2004;207(Pt 18):3189–3200. [PubMed: 15299040]
- Greenamyre JT, Hastings TG. Biomedicine. Parkinson's--divergent causes, convergent mechanisms. *Science* 2004;304(5674):1120–1122. [PubMed: 15155938]
- Grunblatt E, Mandel S, Jacob-Hirsch J, Zeligson S, Amariglio N, Rechavi G, Li J, Ravid R, Roggendorf W, Riederer P, Youdim MB. Gene expression profiling of parkinsonian substantia nigra pars compacta; alterations in ubiquitin-proteasome, heat shock protein, iron and oxidative stress regulated proteins, cell adhesion/cellular matrix and vesicle trafficking genes. *J Neural Transm* 2004;111(12):1543–1573. [PubMed: 15455214]
- Grunblatt E, Mandel S, Maor G, Youdim MB. Gene expression analysis in N-methyl-4-phenyl-1,2,3,6-tetrahydropyridine mice model of Parkinson's disease using cDNA microarray: effect of R-apomorphine. *J Neurochem* 2001;78(1):1–12. [PubMed: 11432968]
- Grunewald T, Beal MF. NOS knockouts and neuroprotection. *Nat Med* 1999;5(12):1354–1355. [PubMed: 10581072]
- Hattori N, Mizuno Y. Pathogenetic mechanisms of parkin in Parkinson's disease. *Lancet* 2004;364(9435):722–724. [PubMed: 15325839]
- Holtz WA, O'Malley KL. Parkinsonian mimetics induce aspects of unfolded protein response in death of dopaminergic neurons. *J Biol Chem* 2003;278(21):19367–19377. [PubMed: 12598533]
- Hur J, Chesnes J, Coser KR, Lee RS, Geck P, Isselbacher KJ, Shioda T. The Bik BH3-only protein is induced in estrogen-starved and antiestrogen-exposed breast cancer cells and provokes apoptosis. *Proc Natl Acad Sci U S A* 2004;101(8):2351–2356. [PubMed: 14983013]
- Imam SZ, Newport GD, Duhart HM, Islam F, Slikker W Jr, Ali SF. Methamphetamine-induced dopaminergic neurotoxicity and production of peroxynitrite are potentiated in nerve growth factor differentiated pheochromocytoma 12 cells. *Ann N Y Acad Sci* 2002;965:204–213. [PubMed: 12105096]
- Jayanthi S, Deng X, Noailles PA, Ladenheim B, Cadet JL. Methamphetamine induces neuronal apoptosis via cross-talks between endoplasmic reticulum and mitochondria-dependent death cascades. *FASEB J* 2004;18(2):238–251. [PubMed: 14769818]
- Jenner P. Oxidative stress in Parkinson's disease. *Ann Neurol* 2003;53(Suppl 3):S26–36. [PubMed: 12666096]discussion S36–28
- Johnstone RW, Tommerup N, Hansen C, Vissing H, Shi Y. Mapping of the human PAWR (par-4) gene to chromosome 12q21. *Genomics* 1998;53(2):241–243. [PubMed: 9790775]
- Kanthasamy AG, Kitazawa M, Kanthasamy A, Anantharam V. Role of proteolytic activation of protein kinase Cdelta in oxidative stress-induced apoptosis. *Antioxid Redox Signal* 2003;5(5):609–620. [PubMed: 14580317]
- Kaul S, Anantharam V, Kanthasamy A, Kanthasamy AG. Wild-type alpha-synuclein interacts with proapoptotic proteins PKCdelta and BAD to protect dopaminergic neuronal cells against MPP+-induced apoptotic cell death. *Brain Res Mol Brain Res* 2005;139(1):137–152. [PubMed: 15978696]

- Kaul S, Kanthasamy A, Kitazawa M, Anantharam V, Kanthasamy AG. Caspase-3 dependent proteolytic activation of protein kinase C delta mediates and regulates 1-methyl-4-phenylpyridinium (MPP+)-induced apoptotic cell death in dopaminergic cells: relevance to oxidative stress in dopaminergic degeneration. *Eur J Neurosci* 2003;18(6):1387–1401. [PubMed: 14511319]
- Kitazawa M, Wagner JR, Kirby ML, Anantharam V, Kanthasamy AG. Oxidative stress and mitochondrial-mediated apoptosis in dopaminergic cells exposed to methylcyclopentadienyl manganese tricarbonyl. *J Pharmacol Exp Ther* 2002;302:26–35. [PubMed: 12065696]
- Kitazawa M, Anantharam V, Kanthasamy AG. Dieldrin induces apoptosis by promoting caspase-3-dependent proteolytic cleavage of protein kinase Cdelta in dopaminergic cells: relevance to oxidative stress and dopaminergic degeneration. *Neuroscience* 2003;119(4):945–964. [PubMed: 12831855]
- Kuhn K, Wellen J, Link N, Maskri L, Lubbert H, Stichel CC. The mouse MPTP model: gene expression changes in dopaminergic neurons. *Eur J Neurosci* 2003;17(1):1–12. [PubMed: 12534964]
- Kweon GR, Marks JD, Krencik R, Leung EH, Schumacker PT, Hyland K, Kang UJ. Distinct mechanisms of neurodegeneration induced by chronic complex I inhibition in dopaminergic and non-dopaminergic cells. *J Biol Chem* 2004;279(50):51783–51792. [PubMed: 15469939]
- Lehrmann E, Hyde TM, Vawter MP, Becker KG, Kleinman JE, Freed WJ. The use of microarrays to characterize neuropsychiatric disorders: postmortem studies of substance abuse and schizophrenia. *Curr Mol Med* 2003;3(5):437–446. [PubMed: 12942997]
- Mandel S, Grunblatt E, Riederer P, Gerlach M, Levites Y, Youdim MB. Neuroprotective strategies in Parkinson's disease : an update on progress. *CNS Drugs* 2003a;17(10):729–762. [PubMed: 12873156]
- Mandel S, Grunblatt E, Riederer P, Youdim MB. Genes and oxidative stress in parkinsonism: cDNA microarray studies. *Adv Neurol* 2003b;91:123–132. [PubMed: 12442671]
- Mandel S, Weinreb O, Youdim MB. Using cDNA microarray to assess Parkinson's disease models and the effects of neuroprotective drugs. *Trends Pharmacol Sci* 2003c;24(4):184–191. [PubMed: 12707005]
- Merghoub T, Gurrieri C, Piazza F, Pandolfi PP. Modeling acute promyelocytic leukemia in the mouse: new insights in the pathogenesis of human leukemias. *Blood Cells Mol Dis* 2001;27(1):231–248. [PubMed: 11358384]
- Miller RM, Callahan LM, Casaceli C, Chen L, Kiser GL, Chui B, Kaysser-Kranich TM, Sendera TJ, Palaniappan C, Federoff HJ. Dysregulation of gene expression in the 1-methyl-4-phenyl-1,2,3,6-tetrahydropyridine-lesioned mouse substantia nigra. *J Neurosci* 2004;24(34):7445–7454. [PubMed: 15329391]
- Miller RM, Federoff HJ. Microarrays in Parkinson's disease: a systematic approach. *NeuroRx* 2006;3(3):319–326. [PubMed: 16815215]
- Moore DJ, West AB, Dawson VL, Dawson TM. Molecular pathophysiology of Parkinson's disease. *Annu Rev Neurosci* 2005;28:57–87. [PubMed: 16022590]
- Moscat J, Diaz-Meco MT. Par-4 keeps the atypical PKCs at bay. *Cell Cycle* 2003;2(2):71–72. [PubMed: 12695647]
- Napolitano M, Centonze D, Calce A, Picconi B, Spiezia S, Gulino A, Bernardi G, Calabresi P. Experimental parkinsonism modulates multiple genes involved in the transduction of dopaminergic signals in the striatum. *Neurobiol Dis* 2002;10(3):387–395. [PubMed: 12270699]
- Nesic O, Svrakic NM, Xu GY, McAdoo D, Westlund KN, Hulsebosch CE, Ye Z, Galante A, Soteropoulos P, Tolias P, Young W, Hart RP, Perez-Polo JR. DNA microarray analysis of the contused spinal cord: effect of NMDA receptor inhibition. *J Neurosci Res* 2002;68(4):406–423. [PubMed: 11992467]
- Nicotra A, Parvez S. Apoptotic molecules and MPTP-induced cell death. *Neurotoxicol Teratol* 2002;24(5):599–605. [PubMed: 12200191]
- Nishi A, Bibb JA, Matsuyama S, Hamada M, Higashi H, Nairn AC, Greengard P. Regulation of DARPP-32 dephosphorylation at PKA- and Cdk5-sites by NMDA and AMPA receptors: distinct roles of calcineurin and protein phosphatase-2A. *J Neurochem* 2002;81(4):832–841. [PubMed: 12065642]
- Ostrerova N, Petrucelli L, Farrer M, Mehta N, Choi P, Hardy J, Wolozin B. alpha-Synuclein shares physical and functional homology with 14-3-3 proteins. *J Neurosci* 1999;19(14):5782–5791. [PubMed: 10407019]

- Pietro RD, Zauli G. Emerging non-apoptotic functions of tumor necrosis factor-related apoptosis-inducing ligand (TRAIL)/Apo2L. *J Cell Physiol* 2004;201(3):331–340. [PubMed: 15389537]
- Prasad KN, Clarkson ED, La Rosa FG, Edwards-Prasad J, Freed CR. Efficacy of grafted immortalized dopamine neurons in an animal model of parkinsonism: a review. *Mol Genet Metab* 1998;65(1):1–9. [PubMed: 9787089]
- Przedborski S, Vila M. The 1-methyl-4-phenyl-1,2,3,6-tetrahydropyridine mouse model: a tool to explore the pathogenesis of Parkinson's disease. *Ann N Y Acad Sci* 2003;991:189–198. [PubMed: 12846987]
- Ricciarelli R, d'Abramo C, Massone S, Marinari U, Pronzato M, Tabaton M. Microarray analysis in Alzheimer's disease and normal aging. *IUBMB Life* 2004;56(6):349–354. [PubMed: 15370883]
- Singh JK, Dasgupta A, Adayev T, Shahmehdi SA, Hammond D, Banerjee P. Apoptosis is associated with an increase in saturated fatty acid containing phospholipids in the neuronal cell line, HN2-5. *Biochim Biophys Acta* 1996;1304(3):171–178. [PubMed: 8982263]
- Strack S, Cribbs JT, Gomez L. Critical role for protein phosphatase 2A heterotrimers in mammalian cell survival. *J Biol Chem* 2004;279(46):47732–47739. [PubMed: 15364932]
- Tan JM, Dawson TM. Parkin blushed by PINK1. *Neuron* 2006;50(4):527–529. [PubMed: 16701203]
- Tatton WG, Chalmers-Redman R, Brown D, Tatton N. Apoptosis in Parkinson's disease: signals for neuronal degradation. *Ann Neurol* 2003;53(Suppl 3):S61–70. [PubMed: 12666099]discussion S70–62
- Thomas GM, Hagan RL. MAPK cascade signalling and synaptic plasticity. *Nat Rev Neurosci* 2004;5(3):173–183. [PubMed: 14976517]
- Ubl A, Berg D, Holzmann C, Kruger R, Berger K, Arzberger T, Bornemann A, Riess O. 14-3-3 protein is a component of Lewy bodies in Parkinson's disease-mutation analysis and association studies of 14-3-3 eta. *Brain Res Mol Brain Res* 2002;108(1–2):33–39. [PubMed: 12480176]
- Von Bohlen Und Halbach O. Synucleins and their relationship to Parkinson's disease. *Cell Tissue Res* 2004
- Winter C, Weiss C, Martin-Villalba A, Zimmermann M, Schenkel J. JunB and Bcl-2 overexpression results in protection against cell death of nigral neurons following axotomy. *Brain Res Mol Brain Res* 2002;104(2):194–202. [PubMed: 12225874]
- Wu HY, Tomizawa K, Oda Y, Wei FY, Lu YF, Matsushita M, Li ST, Moriwaki A, Matsui H. Critical role of calpain-mediated cleavage of calcineurin in excitotoxic neurodegeneration. *J Biol Chem* 2004;279(6):4929–4940. [PubMed: 14627704]
- Xu Z, Cawthon D, McCastlain KA, Slikker W Jr, Ali SF. Selective alterations of gene expression in mice induced by MPTP. *Synapse* 2005;55(1):45–51. [PubMed: 15499605]
- Yamashita H, Nishio M, Fujii Y, Iwase H. Dominant-negative Stat5 inhibits growth and induces apoptosis in T47D-derived tumors in nude mice. *Cancer Sci* 2004;95(8):662–665. [PubMed: 15298729]
- Yang Y, Kaul S, Zhang D, Anantharam V, Kanthasamy AG. Suppression of caspase-3-dependent proteolytic activation of protein kinase C delta by small interfering RNA prevents MPP+-induced dopaminergic degeneration. *Mol Cell Neurosci* 2004;25(3):406–421. [PubMed: 15033169]
- Yoo MS, Kawamata H, Kim DJ, Chun HS, Son JH. Experimental strategy to identify genes susceptible to oxidative stress in nigral dopaminergic neurons. *Neurochem Res* 2004;29(6):1223–1234. [PubMed: 15176479]
- Youdim MB. What have we learnt from CDNA microarray gene expression studies about the role of iron in MPTP induced neurodegeneration and Parkinson's disease? *J Neural Transm* 2003;(Suppl 65): 73–88.
- Youdim MB, Grunblatt E, Levites Y, Maor G, Mandel S. Early and late molecular events in neurodegeneration and neuroprotection in Parkinson's disease MPTP model as assessed by cDNA microarray; the role of iron. *Neurotox Res* 2002;4(7–8):679–689. [PubMed: 12709306]
- Zhuang J, Brady HJ. Emerging role of Mcl-1 in actively counteracting BH3-only proteins in apoptosis. *Cell Death Differ* 2006;13(8):1263–1267. [PubMed: 16676002]

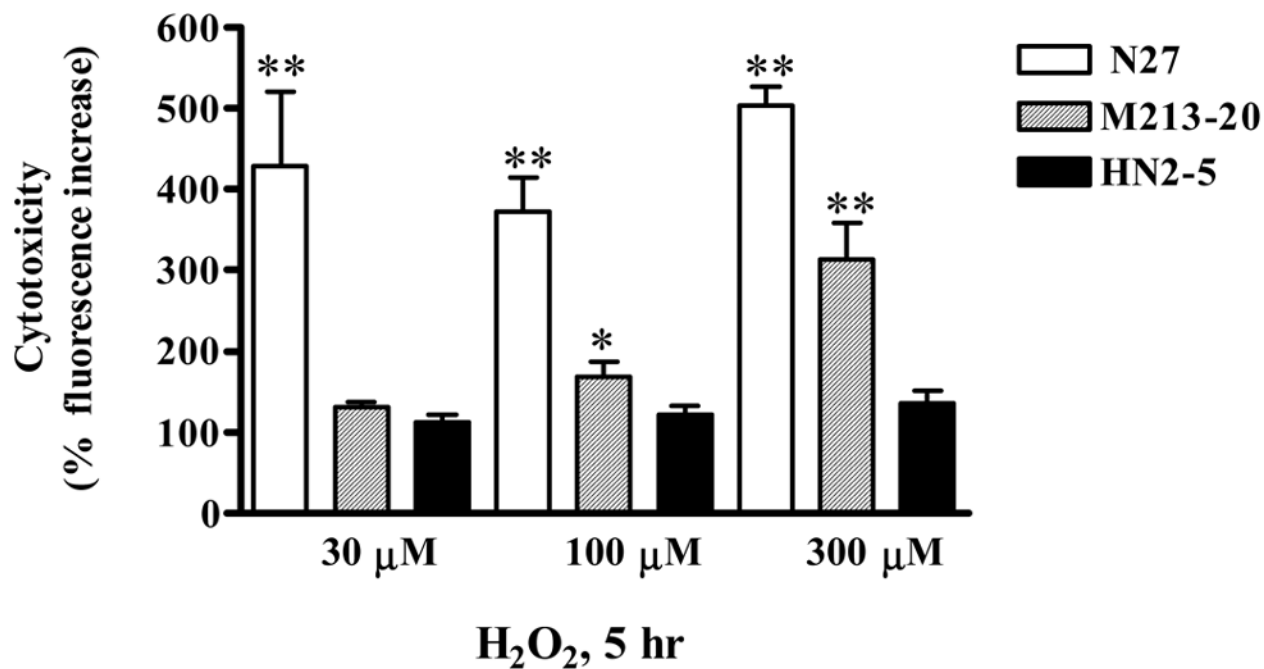


Fig 1. Differential sensitivity of neuronal cell lines to H₂O₂-induced cytotoxic cell death. N27 mesencephalic neuronal cells, M213-20 striatal and HN2-5 hippocampal cells were treated with 30–300 μM H₂O₂ for 5 hr and assayed for cell death with Sytox green assay. Data represent results from eight separate measurements and are expressed as mean ± SEM. Asterisks *p < 0.05 and **p < 0.01 indicates significant differences compared to untreated N27 cells.

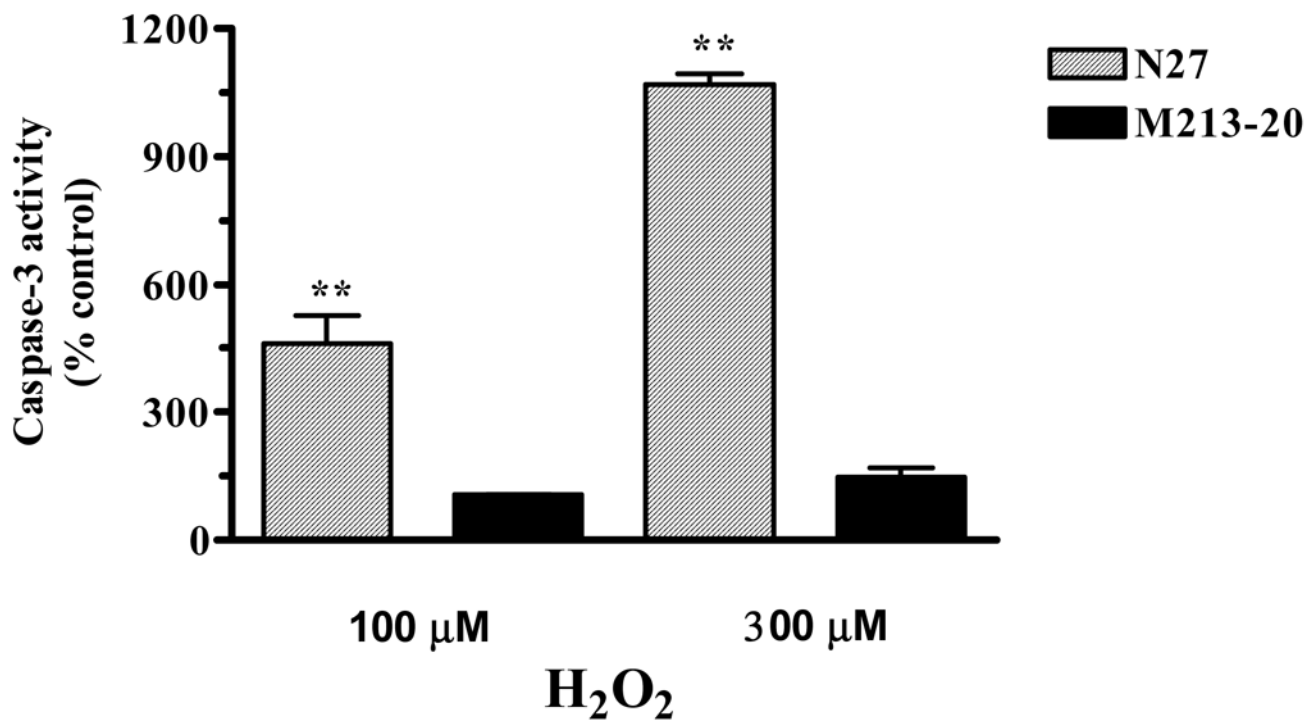
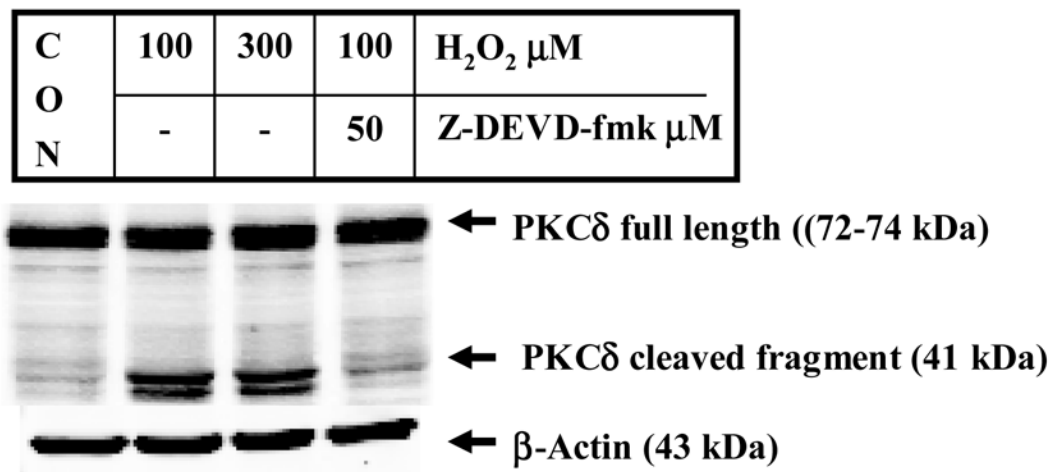


Fig 2. Differential sensitivity of neuronal cell lines to H₂O₂-induced increases in caspase-3 activation. N27 and M213-20 cells were exposed to 100μM or 300μM H₂O₂ for 3 hr at 37 °C. Caspase-3 activity was measured using Ac-DEVD-AMC, as described in the experimental procedures. The data are expressed as % control. Data represent results from five separate measurements and are expressed as mean ± SEM. Asterisks **p<0.01 indicates significant differences compared to untreated N27 cells.

**Fig 3.**

Caspase-3 mediates proteolytic cleavage of PKCδ following exposure of N27 cells to H₂O₂. N27 cells were exposed to 100μM or 300μM H₂O₂ for 4 hr at 37 °C. Cytosolic proteins were collected and resolved by 10% SDS-PAGE, as described in the experimental procedures. In inhibitor studies, cells were pretreated with 50μM Z-DEVD-fmk prior to treatment with 100μM H₂O₂. Arrowheads indicate native PKCδ (72–74 kDa) and cleaved PKCδ fragments (38–41 kDa). To confirm equal protein loading in each lane, the membranes were reprobbed with β-actin antibody. The immunoblots were visualized using ECL detection agents from Amersham.

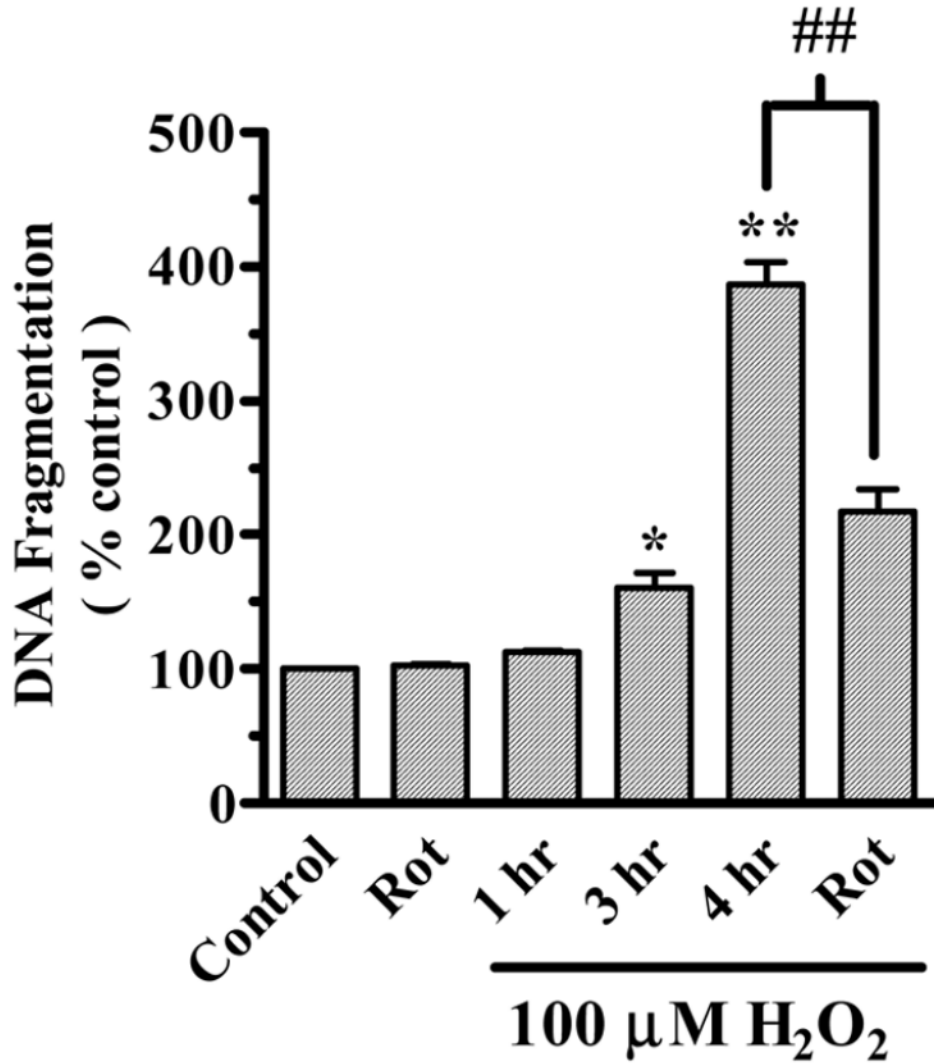


Fig 4.

PKC δ mediates H₂O₂-induced apoptotic cell death. N27 cells were exposed to 100 μ M for 1–4 hr at 37°C. In inhibitor studies, cells were pretreated with 2 μ M rottlerin (Rot) for 30 min prior to treatment with 100 μ M H₂O₂. Cells were lysed after treatment and the extent of DNA fragmentation was determined using a quantitative ELISA assay as described in the experimental procedures. The data are expressed as percentage of apoptosis observed in untreated cells, and represent the mean \pm SEM of six individual measurements. Asterisks (* p <0.05, ** p <0.01) indicate significant differences between untreated and H₂O₂-treated cells. Pound sign (# p <0.01) indicates significant differences between H₂O₂-treated and rottlerin-treated cells.

Table-1

Rat Gene	Accession Number	Direction	5'-3' Nucleotide sequence
GADPH	BC059110	Forward	CAATGCATCCTGCACCACCAAC
		Reverse	CATACTGGCAGGTTTCTCCAG
β-actin	NM_031144	Forward	CCCCTCTGAACCCTAAGG
		Reverse	GAGGTCTTACGGATGTCAA
PAWR	NM_033485	Forward	AGCGAGAGGATGCTATCACA
		Reverse	TAGGGCATCTGTAGGCAACT
PSMD3	XM_213452	Forward	AGAGTTGGAACTGTACCT
		Reverse	AGCTTGCCAGGAACTCGT
CCND1	NM_171992	Forward	TGGATGCTAGAGGTCTGCGA
		Reverse	ACCACACTCCCAGCAGCCA
JUNB	NM_021836	Forward	TCTACACCAACCTCAGCAGT
		Reverse	AGAGTCCAGTGTGTGAGCT
STAT5B	NM_022380	Forward	GAAGCACCTTCAGATCAACCA
		Reverse	AGGATGATGGTCTGCTGCT
MAP2K1	NM_031643	Forward	AGGATGATGGTCTGCTGCT
		Reverse	AGCGAGAGGATGCTATCACA

Table 2








Candidate genes ¹	Accession Number	Human Gene description	Z-Ratio H ₂ O ₂ /Control
Apoptosis			
MCL1	NM_021960	mveloid cell leukemia sequence 1 (BCL2-related)	+ 4.0
BIK	NM_001197	Bcl2-interacting killer (apoptosis-inducing)	+ 4.0
PAWR	NM_002583	apoptosis, WT1, regulator	+ 3.7
PLAGL1	U72621	Pleiomorphic adenoma gene-like1, apoptosis regulator	+ 2.5
DAP	NM_004394	death-associated protein	+ 2.4
ASC	NM_145183	apoptosis-associated speck-like protein containing a CARD	+ 2.3
CASP6	NM_001226	caspase 6, apoptosis-related cysteine protease PRKC,	+ 2.1
BNIP3	NM_004052	BCL2/adenovirus E1B 19kDa interacting protein 3	- 3.8
GLTSCR2	BC013203	glioma tumor suppressor candidate region gene 2	- 2.5
AKT1	NM_005163	v-akt murine thymoma viral oncogene homolog 1	- 2.1
AKT2	AK054771	v-akt murine thymoma viral oncogene homolog 2	- 2.1
BCL2L2	NM_004050	Bcl-2 related protein	- 2.0
Cell cycle and Growth			
CCND1	NM_053056	cyclin D1 (PRAD1: parathyroid adenomatosis 1)	+ 11.7
REPRIMO	NM_019845	candidate mediator of the p53-dependent G2 arrest	+ 4.1
CDC2	NM_001786	cell division cycle 2, G1 to S and G2 to M	+ 3.5
CDC6	NM_001254	cell division cycle 6 homolog (S. cerevisiae)	- 2.1
Chaperones			
CCT7	NM_006429	chaperonin containing TCPI, subunit 7 (eta)	+ 5.9
CSDA	NM_003651	cold shock domain protein A	+ 2.6
HSPA1A	NM_005345	heat shock 70kDa protein 1A	+ 2.5
HSPD1	BC010112	heat shock 60kDa protein 1 (chaperonin)	+ 2.0
14-3-3η	L20422	multifunctional regulatory proteins 14-3-3 family member	- 2.7
HSPA4	AB023420	heat shock 70kDa protein 4	- 2.0
Disease			
EMD	NM_170708	emerin (Emery-Dreifuss muscular dystrophy)	+ 6.1
STK11	NM_000455	serine/threonine kinase 11 (Peutz-Jeghers syndrome)	+ 3.5
DSCR8	BC117304	amyloid beta (A4) precursor protein	+ 2.4
APP	NM_000484	Down syndrome critical region gene 8	+ 2.3
ATM	NM_000051	ataxia telangiectasia	+ 2.0
MADH1	NM_005900	MAD, mothers against decapentaplegic homolog 1	- 3.7
MADH6	NM_005585	MAD, mothers against decapentaplegic homolog 6	- 2.9
WBSCR5	AF252611	Williams-Beuren syndrome chromosome region 5	- 2.1
Mitochondria/Redox			
MCSP	NM_030663	mitochondrial capsule selenoprotein	+ 12.7
ATP5D	BC004426	ATP synthase, H+ transporting, F1 complex, delta subunit	+ 4.0
NDUFS1	BC030833	75 kDa NADH dehydrogenase (ubiquinone) Fe-S protein 1	+ 3.5
TOMM20	NM_014765	translocase of outer mitochondrial membrane 20	+ 2.6
SLC25A15	NM_014252	member mitochondrial carrier; ornithine transporter	- 3.9
UCP3	NM_003356	uncoupling protein 3 (mitochondrial, proton carrier)	- 3.0
MTCH1	NM_014341	mitochondrial carrier homolog 1	- 2.3
Ubiquitin- Proteasome			
PSMD3	NM_002809	proteasome (prosome, macropain) 26S subunit, non-ATPase, 3	+ 3.0
USP4	NM_003363	ubiquitin specific protease 4 (proto-oncogene)	+ 2.0
UBE2J1	BC013973	ubiquitin-conjugating enzyme E2, J1	- 2.5
UBC3B	BC047584	ubiquitin-conjugating enzyme E2R 2	- 2.3
Nuclear/Transcription			
NPAS2	NM_002518	Gas-responsive heme-binding neuronal PAS transcription factor	+ 5.3
USF2	NM_003367	upstream transcription factor 2, c-fos interacting jun B proto-oncogene	+ 5.2
JUNB	NM_002229	oncogene	+ 4.0
STAT5B	NM_012448	Signal transducer and activator of transcription 5B	+ 4.0
ATF4	NM_001675	activating transcription factor 4	+ 3.8
TP53BP2	NM_005426	tumor protein p53 binding protein, 2	+ 3.0
WIG1	AK122768	p53 target zinc finger protein	- 6.5
SUP4H1	NM_003168	suppressor of Ty 4 homolog 1 (S. cerevisiae)	- 5.5
HSF1	NM_005526	heat shock transcription factor 1	- 3.6
TFAP4	NM_003223	transcription factor AP-4 (activating enhancer binding protein 4)	- 3.0
Kinases			
DYRK2	NM_006482	dual-specificity tyrosine-(Y)-phosphorylation regulated kinase 2	+ 4.6
MEKK4	NM_002747	mitogen-activated protein kinase kinase kinase 2	+ 3.8
PHKA2	NM_000292	phosphorylase kinase, alpha 2 (liver)	+ 3.7
STK11	NM_000455	serine/threonine kinase 11 (Peutz-Jeghers syndrome)	+ 3.5
PTK2	AL832961	protein tyrosine kinase 2	+ 2.6
ABL2	NM_005759	abl-tyrosine kinase interactor 2	+ 2.5
CSNK2A2	NM_001896	casein kinase 2, alpha prime polypeptide	- 3.8
STK6	NM_003600	serine/threonine kinase 6	- 3.5
MAP2K1	NM_002755	mitogen-activated protein kinase kinase 1	- 3.2

Candidate genes ¹	Accession Number	Human Gene description	Z-Ratio H ₂ O ₂ /Control
TYK2	NM_003331	tyrosine kinase 2	-2.8
CSNK1E	NM_001894	casein kinase 1, epsilon	-2.3
Phosphatases			
PP2B	NM_005605	protein phosphatase 2B (PPP3CC, calcineurin A gamma)	+3.0
PTPN2	NM_002828	protein tyrosine phosphatase, non-receptor type 2	+2.3
PPM1D	NM_003620	protein phosphatase 1D magnesium-dependent, delta isoform	-4.6
PPP1R8	NM_138558	protein phosphatase 1, regulatory (inhibitor) subunit 8	-3.1
PR48	BC041879	protein phosphatase 2A 48 kDa regulatory subunit	-3.0
PPP5C	NM_006247	protein phosphatase 5, catalytic subunit	-2.8
Ras/Rab related GTPases			
RAB5C	NM_004583	RAB21, member RAS oncogene family	+3.5
RAB21	NM_014999	RAB32, member RAS oncogene family	+3.2
RAB32	NM_006834	RAB5C, member RAS oncogene family	+3.2
RAGA	NM_006570	Ras-related GTP-binding protein	-6.2
RABL2B	NM_007081	RAB, member of RAS oncogene family-like 2B	-5.5
RAB2	NM_002865	RAB2, member RAS oncogene family	-2.7
Others			
SNCB	NM_003085	synuclein, beta	-3.8
NPTXR	NM_014293	Neuronal Pentraxin Receptor, mediates pattern recognition	-3.6
NEUROD1	DQ894747	neurogenic differentiation 1	-3.1
YWHAH	NM_003405	tyrosine 3-monooxygenase/tryptophan 5-monooxygenase	-3.0
MAOB	NM_000898	activation (eta) monoamine oxidase B	-2.2

¹ The candidate genes have been classified into functional groups and were annotated using the GenBank Accession numbers. Z-ratio values $\geq +2.0$ or ≤ -2.0 were chosen as cut-off values, defining increased and decreased expression, respectively (see methods for more details).

Table 3


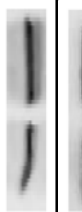
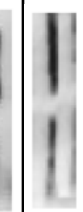
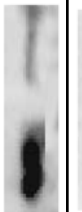
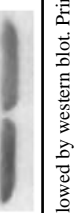

Quantitative RT-PCR analysis of select candidate genes

Genes	Band size (bp)	DNA Gel Con - H ₂ O ₂	H ₂ O ₂ /con mRNA fold difference	Z-Ratio H ₂ O ₂ /Con
CCND1 cyclin D1	720		+ 4.1	+ 11.7
STAT5B Signal transducer and activator of transcription 5B	326		+ 3.0	+ 4.0
Jun B proto-oncogene	630		+ 2.8	+ 4.0
PWR apoptosis, WT1, regulator	852		+ 2.9	+ 3.7
PSMD3 26S proteasome subunit, non- ATPase, 3	976		+ 2.8	+ 3.0
MAP2K mitogen-activated protein kinase kinase 1	1703		- 1.1	- 3.2
GAPDH Glyceral Aldehyde Dehydrogenase	640		+ 1.0	-

Total RNA was extracted from control and H₂O₂-treated N27 cells using the Trizol reagent. RT-PCR was performed using the primers designed against the rat species (see methods section for more details).

Table 4

Western blot analysis of select candidate genes

Genes	Band size (kDa)	Western blot Con - H ₂ O ₂	Protein H ₂ O ₂ /Con fold difference	Z-Ratio H ₂ O ₂ /Con
Jun B proto-oncogene	39		+ 3.0	+ 4.0
STAT5B Signal transducer and activator of transcription 5B	80		+ 2.5	+ 4.0
MEKK4 mitogen-activated protein kinase kinase kinase 2	45		+ 3.6	+ 3.8
PP2B protein phosphatase 2B (calcineurin A gamma)	60		+ 2.3	+ 3.0
BNIP3 BCL2/adenovirus E1B interacting protein 3	19		- 3.0	- 3.8
β-actin	43		+ 1.0	-

Control and H₂O₂-treated cell extracts were separated on 10–15% SDS-PAGE followed by western blot. Primary antibodies that would recognize the rat species were used in this study (see methods section for more details).